Maximizing Throughput via Vertical Optimization of the Coherent MODEM

R. Maher, M. Torbatian, A. Nguyen, Z. Wang, S. Koenig, M. Missey, A. Le Liepvre, R. Going, S. Wolf, P. Samra, P. Day, S. Tremblay, M. Ziari, F. Kish, S. Sanders, P. Kandappan

Infinera Corporation, Sunnyvale, CA 94089, USA
**rmaher@infinera.com*

Abstract: Vertical optimization of DSP algorithms, analog electronics, optical components and PCB design is critical to maximize the SNR limit of the digital coherent MODEM. We demonstrate a record net ISD of 10.82b/s/Hz for a vertically optimized 256QAM transceiver operating at a symbol rate >50GBd.

OCIS codes: (060.1660) Coherent communications; (060.4080) Modulation.

1. Introduction

As the symbol rates of commercialized line cards approach 100 GBd, vertical optimization of the coherent MODEM, where the constituent components of the digital coherent transceiver are co-designed, has become a pre-requisite in order to maintain the SNR limit required to enable higher order modulation formats, such as 64QAM[1]. There are many examples of co-dependent design choices that can lead to a detrimental impact on the transceiver SNR limit if made in isolation, such as the trade-off between the cycle slip rate (and power consumption) of the carrier phase estimation algorithm and laser phase noise, the return loss of each radio frequency (RF) transition in the RF path and the capability of the triple transit reflection (TTR) mitigation filters in the digital signal processing (DSP) application specific integrated circuit (ASIC) or the ability to track over-life signal impairments, like transmitter skew.

In this work, we demonstrate the performance of a vertically optimized integrated digital coherent optics (DCO) module in a live production network. The DCO is comprised of four DSP ASICs and a 4-CH optical module, which includes photonic integrated widely tunable lasers (WTL), Mach-Zehnder modulator driver (MZMD) arrays, dual polarization IQ MZMs and a full coherent receiver that incorporates a trans-impedance amplifier (TIA) and automatic gain control (AGC) circuit array[2]. The DCO module, operated in offline mode, is used to transmit and receive a single carrier 57.8 GBd PS-256QAM signal over an installed 53 km optical link. A record information spectral density (ISD) of 10.82 b/s/Hz was achieved after transmission for a DCO module operating at a symbol rate > 50 GBd.

2. DCO Module

Fig. 1 (a) illustrates the real-time 4-CH 68.9 GBd DP-64QAM (600 Gb/s per wavelength) DCO module used in this work[3]. The DCO connects four 16 nm DSP ASICs to individual transmitter (TX) and receiver (RX) optical modules. The TX module consists of a 4-CH dual-polarization Indium Phosphide (InP) based photonic integrated circuit (PIC), hybrid integrated with an ultra linear 180 nm SiGe BiCMOS MZMD array. The RX module also consists of a 4-CH InP based PIC, hybrid integrated with a 180 nm SiGe BiCMOS TIA/AGC array. Each WDM channel and local oscillator on the PIC comprises a WTL with linewidth < 100 kHz, allowing continuous tuning over the extended C-band (4.8 THz)[4]. The real time DSP ASIC contains on-chip memory just before the digital-to-analog converter (DAC) and after the analog-to-digital converter (ADC). Therefore, it can be operated in offline mode, allowing for arbitrary patterns to be loaded onto the DAC, transmitted over the channel and recorded by the ADC at the receiver. This feature enables the evaluation of PS-256QAM using a generic DSP implementation, carried out offline in MATLAB.

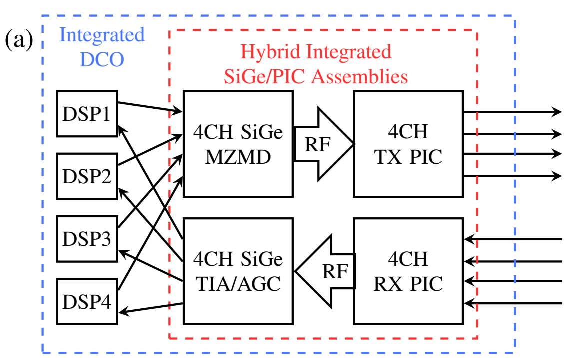

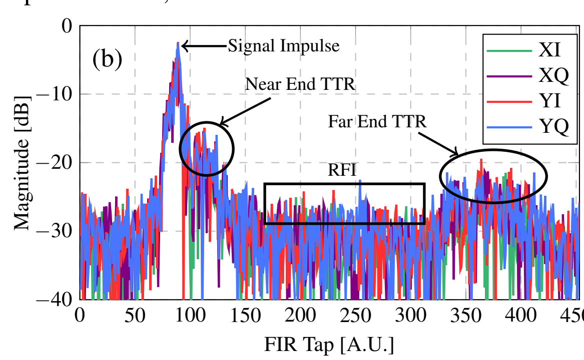

Fig. 1: (a) 4-CH integrated DCO. (b) Filter taps from the TTR mitigation filters for the XI, XQ, YI and YQ RF paths.

Fig. 1 (b) shows the time domain taps from the TTR mitigation filter used to correct receiver side reflections that occur between the DSP ASICs and the hybrid integrated SiGe/PIC assemblies. The main signal impulse response is observed at tap number 89, which is followed by near end TTRs that occur between the DSP ASIC package and the RF interconnect (RFI). The filter response is sparse during the round-trip propagation delay of the RFI, which is followed by the far end TTRs arising from the transition to the hybrid integrated SiGe/PIC assemblies. Through vertical optimization of the DCO, the signal integrity of the entire RF chain was carefully engineered, such that the triple transit delay and the magnitude of the reflections could be mitigated using a co-designed digital mitigation filter, in order minimize the SNR penalty due to RF reflections. This optimization is one example of many co-dependent design choices required to maximize the SNR limit of the digital coherent MODEM.

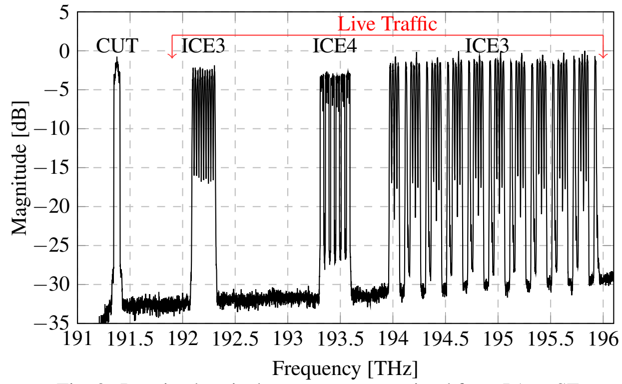

Fig. 2: Received optical spectrum, transmitted from PA to SF.

3. FEC and PS Encoder/Decoder Implementation

The constellation shaped symbols used in this work were generated using probabilistic amplitude shaping (PAS)[5], which was implemented using a distribution matching (DM) algorithm similar to constant composition DM (CCDM)[6]. A single circuitry was used to support an IR range from 5 to 8 b/sym/pol by varying the symbol probability distributions[7]. At the TX, the shaped amplitude levels for the in-phase and quadrature dimensions of each polarization were generated by the DM and the corresponding binary representations were subsequently passed to the FEC engine, which consisted of an outer hard decision code and an inner soft decision code with a total code rate of 0.833. The output bits from the FEC encoder were passed through an interleaver, which both preserved the desired symbol distribution and reduced the probability of burst errors after decoding in the receiver. The parity bits of the FEC encoder and additional information bits were paired with the amplitude levels generated by the DM encoder and fed into the symbol mapper.

The shaped symbols were 1.5 times over sampled, before being spectrally filtered using a root raised cosine (RRC) filter with a roll-off factor of 0.05. The signals were pre-emphasized to mitigate the non-ideal bandwidth (BW) response of the TX RF signal path, with the filter also mitigating for triple transit reflections (TTR). The signals were subsequently loaded onto the DSP ASIC DAC memory and transmitted over the live network. At the receiver, the symbols were captured from the ADC memory in the DSP ASIC and exported to MATLAB. A static post-emphasis digital filter corrected both the non-ideal BW response and TTRs generated within the receiver (shown in Fig. 1 (b)). The remaining DSP blocks consisted of signal normalization, DC offset removal, RX de-skew, hybrid angle error correction, chromatic dispersion compensation, matched filtering and data aided adaptive equalization (tap pre-convergence followed by pilot insertion with rate 32/33 for DA update). Carrier phase estimation was carried out using a maximum likelihood feed forward carrier recovery algorithm and was followed by an adaptive least mean square (LMS) equalizer to mitigate TX skew and MZM quadrature error. The log likelihood ratios (LLR) were calculated from the symbols at the output of the LMS equalizer before being de-interleaved and passed into the binary FEC decoder. The subsequent decoded sign and amplitude bits were separated, with the latter being passed into the DM decoder, which recovered the original information bits. This procedure was repeated for 9 FEC frames and the resulting information bits were used to calculate the bit error ratio (BER), frame error rate (FER) and Q^2-factor.

4. Results and Discussion

A 53 km optical link connecting sites in San Francisco (SF) and Palo Alto (PA) was selected from Telia Carrier's North American backbone fiber network for the live field trial. Both locations feature a wavelength selective switch (WSS) based re-configurable optical add-drop multiplexer, which was used to add and drop a single channel under test (CUT) at each site. The line system considered the optical carrier as an alien wave and automatically adjusted the launch power onto the line, based on the spectrum allocated by the WSS (100 GHz). During the field demonstration, live customer traffic remained present on the network and was not impacted by the insertion or removal of the CUT. Fig. 2 illustrates the received optical spectrum at the SF site. The 57.8 GBd PS-256QAM optical carrier operated at a lasing frequency of 191.3 THz, while live customer traffic from various nodes within the North American network covered the remainder of the C-band, with ICE3 and ICE4 (Infinera's 3rd and 4th generation) real-time line cards transporting 16 GBd DP-QPSK and 32 GBd DP-16QAM super-channels, respectively. Fig. 3 (a) shows the entropy

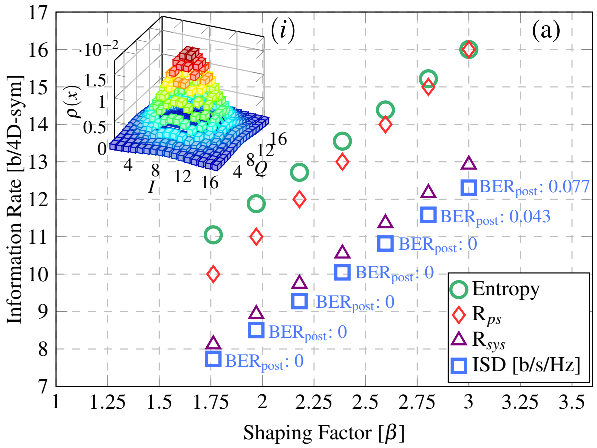

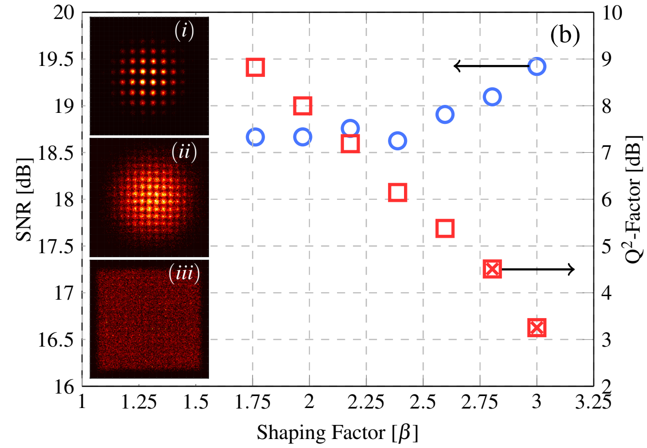

Fig. 3: (a) Entropy, R_{ps}, R_{sys}, ISD and corresponding post-FEC BER after transmission. Inset (*i*): symbol probabilities for a shaping factor of 2.6. (b) SNR and Q^2-factor as a function of β. Insets (*i*), (*ii*) and (*iii*): constellations for β values of 1.76, 2.6 and 3, respectively.

rate (b/4D-sym) of each symbol distribution used in transmission, as a function of the PS shaping factor (β). While the entropy rate defines the maximum IR for a given symbol distribution, β (entropy of 1D symbol amplitude probabilities) provides insight into the strength of the shaping itself. For example, $\beta = 3$, is equivalent to uniform 256QAM, while $\beta = 0$, is equivalent to QPSK. The achieved information rate using our FEC and PS encoder/decoder scheme, R_{ps}, was equivalent to entropy for uniform 256QAM, however as β decreased, R_{ps} diverged from entropy due to the use of a non-ideal fixed length DM. The rate loss of the DM dictates that the base constellation should be reduced for very strongly shaped distributions in order to maximize R_{ps}. The IR of the overall system (R_{sys}) incorporates the FEC OH and pilot OH, while the ISD takes the RRC filter roll-off into account and represents the maximum single channel spectral efficiency. For uniform 256QAM ($\beta = 3$), R_{sys} of 12.92 b/sym, ISD of 12.31 b/s/Hz and a net bit rate of 747 Gb/s was achieved after transmission over the link. However, the post-FEC BER (BER_{post}) was 0.077 and the FER was 1, therefore β was reduced until the BER_{post} was 0. This was realized at a shaping factor of 2.6, thus achieving a record ISD of 10.82 b/s/Hz for a PS-256QAM optical channel at a symbol rate > 50 GBd (corresponding net bit rate of 657 Gb/s). For all subsequent values of $\beta < 2.6$, post-FEC error free transmission was achieved.

The excess system margin as a function of shaping factor can be visualized in Fig. 3 (b). At $\beta = 3$, a SNR of 19.4 dB and Q^2-factor of 3.25 dB was recorded, however as mentioned previously, the BER_{post} was non-zero (as indicated by the x mark in Fig. 3 (b)). As β was reduced, the Q^2-factor increased, reaching 5.3 dB for a shaping factor of 2.6 and an ISD of 10.82 b/s/Hz. This performance was very close to the FEC threshold, therefore if additional WDM channels were loaded onto this portion of the network, a BER_{post} of 0 may not be possible (due to additional linear or non-linear penalties). In such a scenario, β could be reduced in order to trade-off ISD in favor of improved system margin. This is demonstrated by reducing β down to 1.76, which decreased the ISD to 7.74 b/s/Hz and increased the Q^2-factor to 8.8 dB, thus providing a large system margin to the FEC threshold, which could be used for greater transmission reach or tighter channel spacing. This very high level of system performance using an integrated DCO module demonstrates the benefit of vertical optimization of the coherent MODEM and the applicability of high symbol rate, high order PS-QAM formats in existing short reach optical networks.

Acknowledgments
The authors would like to thank Telia Carrier for providing access to their North American fiber network.

References

1. R. Maher *et al.*, "Increasing the information rates of optical communications via coded modulation: a study of transceiver performance," Sci. Rep., vol. **6**, 21278, 2016.
2. R. Going *et al.*, "4 x 600 Gb/s photonic IC transmitter and receiver modules," in European Conference on Optical Communication (ECOC), Mo4C.1, 2018.
3. R. Maher *et al.*, "Constellation shaping for high symbol rate SNR limited transceivers," in SPIE Photonics West, Proceedings Volume 10947, Next-Generation Optical Communication: Components, Sub-Systems, and Systems VIII; 1094708, 2019.
4. R. Going *et al.*, "1.00 (0.88) Tb/s per wave capable coherent multi-channel transmitter (receiver) InP-based PICs with hybrid integrated SiGe electronics," IEEE J. Quantum Electron., vol. **54**, 8000310, 2018.
5. F. Buchali *et al.*, "Rate adaptation and reach increase by probabilistically shaped 64-QAM: An experimental demonstration," J. Lightw. Technol., vol. **34**, pp. 1599, 2016.
6. P. Schulte and G. Böcherer, "Constant composition distribution matching," IEEE Trans. Inf. Theory., vol. **62**, pp. 430, 2016.
7. F.R. Kschischang and S. Pasupathy, "Optimal nonuniform signaling for Gaussian channels," IEEE Trans. Inf. Theory., vol. **39**, pp. 913, 1993.